

ENGINEERING RESEARCH INSTITUTE  
UNIVERSITY OF MICHIGAN  
ANN ARBOR

QUARTERLY PROGRESS REPORT NO. 5

AN INVESTIGATION OF INTERGRANULAR OXIDATION  
IN STAINLESS STEEL

M. J. SINNOTT

C. A. SIEBERT

R. E. KEITH

L. H. DeSMYTER

Project 2110

DEPARTMENT OF THE AIR FORCE  
WRIGHT AIR DEVELOPMENT CENTER  
WRIGHT-PATTERSON AIR FORCE BASE  
CONTRACT NO. AF33(616)-353, PROJECT NO. 54-670-60

October, 1954

## TABLE OF CONTENTS

	Page
INTRODUCTION	1
MATERIAL	1
EQUIPMENT	1
PROCEDURE	2
Unstressed Oxidation	2
Stressed Oxidation	2
Weight Gain	2
Electron Diffraction	2
RESULTS AND DISCUSSION	4
Stressed Oxidation	4
X-ray Results	5
Electron Diffraction	5
Unstressed Oxidation	7

AN INVESTIGATION OF INTERGRANULAR OXIDATION IN STAINLESS STEEL

INTRODUCTION

This research project has been undertaken under the sponsorship of Wright Air Development Center of the U.S. Air Force. Its objectives are:

- (a) to determine the effect of temperatures between 1600° and 2000°F on intergranular oxidation,
- (b) to examine the effects of alloy composition on intergranular oxidation,
- (c) to determine the nature of the penetrating material in areas of intergranular attack, and
- (d) to devise methods of reducing or eliminating intergranular penetration.

MATERIAL

The materials used during this phase of the investigation were chromel alloy (ARM, heats A and B), chromel alloy D, the type 310 stainless steels used in the previous years work (WADC TR 54-120), vacuum melted type 310 stainless steel, and inconel. An analysis of these alloys is given in Table I.

EQUIPMENT

The equipment used for the stressed oxidation is the same as mentioned in the June, 1954, Progress Report, 2110-3-P.

A humidifying unit has been constructed (Fig. 1) and is at present undergoing testing. By proper blending of dry air and humid air, atmospheres over a wide range of dewpoints can be generated.

Equipment has been constructed to measure the weight gained during oxidation (Fig. 2). The sample 2" x 1" is suspended from an arm of an analytical chainomatic balance by a platinum wire and oxidized in the furnace. Dried air (dewpoint <-40) is preheated over broken ceramic in the bottom of the furnace and passed over the sample with a velocity of 30 ft/min.

### PROCEDURE

#### Unstressed Oxidation

The unstressed oxidation procedure has been completely described in last years final report (WADC TR 54-120).

#### Stressed Oxidation

The specimens are subjected to oxidation at varying temperature and stress levels in the apparatus described in Progress Report 2110-3-P. Both ends of the furnace are partially open and air reaches the specimen by convection. The 2-inch test section of the specimen is subjected to the same preparation and counting procedure as the unstressed specimens.

#### Weight Gain

The unit (Fig. 2) is loaded by suspending the sample from the end of the platinum wire and lowering the suspension into the furnace. The sample is weighed every hour during the first few hours of the test and three times daily for the remainder of the test. After the weight gain has been determined the samples are treated as unstressed oxidation specimens and the penetration data taken.

#### Electron Diffraction

In an effort to determine the nature of the intergranular compounds, a technique was developed for examining the subsurface regions of oxidized specimens by means of reflection electron diffraction, a method well suited for the study of solid surface layers. The procedure which was followed on previously oxidized specimens consisted of the following steps:

- (1) All the external scale possible was removed by scraping, without actually disturbing the metal surface itself. The scale thus collected was powdered and analyzed by x-ray diffraction using the same technique described previously (WADC TR 54-120).

- (2) Thickness measurements were made on the specimen at two points on the surface. One of these points was later to be subject to etching action while the other was to be protected from etching by Scotch tape, and thus, served as a reference standard for later thickness measurements. These measurements were made on a Pratt and Whitney supermicrometer accurate to 0.0001 inch. The assumption was that the etching attack on the exposed underside of the specimen was essentially uniform.
- (3) An electron-diffraction pattern was made of the specimen surface, using an RCA Type EMD-2 electron diffraction apparatus.
- (4) The specimen was electrolytically etched for 15 to 30 sec. in a mixture of 10 percent perchloric acid and 90 percent glacial acetic acid at a temperature of 15° C and a current density of 6 amp/in.<sup>2</sup>. This etching treatment has the property of removing the metal without disturbing the intergranular compounds.\*
- (5) An electron diffraction pattern was made of the exposed compounds.
- (6) The exposed compounds were brushed off the surface using a rotary wire brush on a hand-power tool. The brush did not damage the surface, and in addition, was much less likely to cause contamination than was an abrasive compound. The Scotch tape covering the unetched portion of the specimen was then removed.
- (7) Thickness measurements were made of the etched and unetched portions of the specimen as described in Step 2. By appropriate subtractions, the amount of metal removed in the etching operation could then be determined. A fresh piece of Scotch tape was then applied to the unetched portion of the surface and Steps 4 through 7 were repeated as many times as necessary to reach the depth in the specimen where diffraction patterns from the intergranular compounds no longer appeared.

The electron diffraction procedure outlined above made it possible to show any changes in the overall composition of the intergranular compounds resulting from oxidation as a function of their depth below the

---

\* Brockway, L.O. and Bigelow, W.C., "Development of Procedure for the Identification of Minor Phases in Heat Resistant Alloy by Electron Diffraction", Annual Summary Report on Project 2020, Eng. Res. Inst., Univ. of Mich., to Flight Research Laboratory (WCRRL), WADC, 15 January 1953.

metal-oxide interface. For this part of the program, six heats were selected from the nine studied in the oxidation runs. These heats were: type 309 plus Nb and type 310 heats 64177, 64270, X11306, X11338, and X27258. The other three type 310 heats were similar in their penetration characteristics to heat X27258 and the latter heat was taken as being representative of them also. In the case of the type 309 plus Nb and type 310 heats 64177, and 64270, specimens were studied following 100 hours oxidation at 1600°, 1700°, 1800°, and 1900°F. For the heats X11306, X11338, and X27258, 2000°F specimens were studied in addition to the other four temperatures.

In connection with the electron diffraction studies, it should be mentioned that this method also has its limitations, although it is capable of use with extremely small amounts of materials and is especially useful for thin films. The smallest uncertainty in interplanar spacing which can be expected using the reflection electron-diffraction technique is about 2 percent. Since this uncertainty is of the same order as the change in interplanar spacing between the diffraction patterns of  $\text{Fe}_2\text{O}_3$  and  $\text{Cr}_2\text{O}_3$ , and between spinels having low and high lattice parameters, the electron diffraction studies can do little more in the present case than to indicate the presence or absence of the rhombohedral or cubic phases.

In evaluating the diffraction patterns obtained, the relative proportions of spinel and rhombohedral phases shown in individual patterns were indicated by specifying whether the patterns of specific phases were strong (S), medium (M), weak (W), very weak (VW), or very, very weak (VVW) (see Table II). In addition, a qualitative attempt was made to show the diminution of diffracted intensity from intergranular oxides on individual specimens accompanying successive etches by referring intensities to those obtained in patterns taken prior to etching. It must be borne in mind, however, that comparison of relative intensities obtained in different exposures can be misleading, since many factors related to exposure and specimen surface preparation and alignment can influence the intensity obtained in a given pattern and these factors vary among exposures.

## RESULTS AND DISCUSSION

### Stressed Oxidation

To date, results have been obtained on the chromel alloy ARM Heat A at temperatures of 1800, 1900, and 2000°F. The stresses used are a function of the temperature. The number of penetrations versus depth at constant stress and temperature is given in Figs. 19 through 21. These curves follow the general decay-type curves observed in the unstressed studies. Figures 22 through 27 show the variation in number and mean depth at constant temperature.

The general trend is for the number of penetrations to remain fairly constant with increasing stress until the elongation becomes measureable, at which time the number of penetrations increases. The number of penetrations increases with increasing stress and consequent elongation until a discontinuity appears where the material begins to tear due to the first stages of rupture. Figure 3 is a typical specimen which exhibited fissures throughout the matrix. Some of the tears show very little oxide, indicating that oxidation was not directly responsible. An unidentified phase is present in the structure shown in Figs. 3 and 4. This may be chromium nitride. An attempt will be made to identify this in the near future. Since this phase is harder than the matrix it shows up as a relief constituent on polishing and therefore an etch was not required in this photomicrograph.

The mean depth of penetration is slightly lower when a low stress is applied than for the unstressed condition shown in Figs. 23, 25, and 27. Although this decrease in depth of penetration is slight, it is consistent in all instances. However, there is a tendency for the mean depth of penetration to increase with increasing stress which is accompanied by an increase in elongation of the test specimens. Figures 11 and 12 show the type penetrations developed in the chromel material at 2000°F and stresses of 250 and 500 psi. The 250 psi stress is the lowest stress used, while the stress of 500 psi represents a level which resulted in considerable elongation and increase in penetration depth. The unstressed specimens were run in dry air ( $D_p < 40^\circ\text{F}$ ) and the stressed specimens in undried air ( $D_p > 40^\circ\text{F}$ ). The presence of more water vapor in the air flowing past the stressed specimens may have caused a slightly greater volume of oxidation, which would result in a decrease in intergranular oxidation.

A vertical dotted line in Figs. 22 through 27 indicates the stress level at which internal fissuring was first observed throughout the specimen as shown in Figs. 3 and 4.

### X-ray Results

X-ray diffraction patterns have been obtained on most of the oxides and are in the process of interpretation.

### Electron Diffraction

One of the objectives of this investigation was to attempt to determine the nature of the intergranular material extending into the metal from the scale layer. It was desired to find the composition of this material and whether there were any significant differences between its composition and that of the external scale material. Just how this was to be done experimentally was something of a problem, since the intergranular material was well dispersed and extremely thin. The method ultimately adopted was described in the Procedure section, and utilized reflection electron diffraction following successive etching treatments. Using this technique, it was possible to obtain data on the composition of the intergranular material as a function of depth below the metal-oxide interface. The

results obtained by this method are presented in Table II. Six heats of material were selected for examination; type 309 plus Nb and type 310 heats 64177, 64270, X11306, X11338, and X27258. Specimens from the latter three heats were examined at all temperatures of oxidation, while the first three heats were examined only at the four lower temperatures. The program was restricted to an oxidation time of 100 hours.

As was noted previously, the accuracy obtainable with the reflection electron-diffraction technique is of the order of 1 or 2 percent error in interplanar spacing, the same order as the changes in lattice parameters between  $\text{Cr}_2\text{O}_3$  and  $\text{Fe}_2\text{O}_3$  and between spinels having the highest and lowest possible lattice parameters. Therefore, the phases shown to be present in the electron diffraction patterns could be identified only as "rhombohedral" or "spinel". Examples of these two patterns are presented in Figs. 5 and 6. Identification was made on the basis of the (220) spinel line and several rhombohedral lines, notably the (100), (110), (120), and (200) lines. The appearance of the (100) line in the electron diffraction patterns could be due either to oriented oxide growth or to the fact that the low-angle structure factor for electrons is greater than for x-rays. The latter reason is the more likely, considering the probable randomness of the surface-metal grain orientations.

The electron-diffraction results showed that the same phases exist in the grain boundary fissures as were found in the external scales. In heats 64177 and 64270 the spinel phase was rarely observed. In the other four heats both phases appeared, the spinel phase being especially prominent in the type 309 plus Nb alloy with its high Mn content (see Table I). The relative proportions of the phases in a given specimen seemed to vary slightly with depth but the two patterns taken on each specimen at the same depth often showed similar variations. As nearly as can be determined, the intergranular material is identical to the material found in the external scale and is in general simply an inward extension of the external scale.

In order to be absolutely certain that the electron-diffraction patterns obtained were not from reaction products between the metal and the etchant, a specimen was etched and allowed to dry without rinsing. The resulting electron-diffraction pattern could be easily differentiated from those associated with the two oxide phases obtained by the routine process.

Figures 7 through 10 show the metallographic appearance of the specimen surfaces following successive etching treatments. The photomicrographs were taken using oblique light in order to show the oxides in relief more clearly. These photomicrographs show that electrolytic etching with 10 percent perchloric acid and 90 percent glacial acetic acid left the intergranular oxide films intact and exposed. Figures 7 through 10 also illustrate something which was observed at the time etching was carried out; namely, that the first etching usually attacked the metal only at certain points where the path through the surface scale to the metal was relatively open. Further etching undercut the scale layer adjacent to these points and in the subsequent brushing process new metal



surface was exposed. Ultimately, the scale layer could be completely removed by this process, but at the same time much of the deeper intergranular material in the areas which etched initially was probably lost. Furthermore, patterns taken while appreciable amounts of scale remained on the surface probably are not representative of intergranular material at all, since the scale would serve to block the intergranular material from the electron beam. In some specimens no difficulty was encountered with adhering scales and even the first patterns obtained are representative of intergranular material.

It will be noted from Table II, when compared with the appropriate penetration versus depth curves, that the measured depths below which no oxide patterns were obtained were sometimes very much less than the maximum fissure depths observed metallographically. In a few cases apparent increases in thickness of the metal were observed on etching. There are two alternative conclusions that can be drawn from these facts; either the thickness measurements as made on the super-micrometer were not as reliable as they were believed to be, or the number of intergranular oxide areas in relief at the deeper levels was not sufficient to give an electron-diffraction pattern. Considering the apparent thickness increases on some specimens and the sensitivity of the electron-diffraction technique, the probability is that the measurements were not representative. Since the surfaces often became rather rough as a result of the etching treatment, it was difficult to devise a suitable means of making thickness measurements which would be accurate to 0.0001 inch and at the same time would be representative of the surface as a whole.

#### Unstressed Oxidation

Chromel alloys (ARM heat A and B) and D were tested at 1600, 1700, 1800, 1900, and 2000°F in the unstressed condition. The air velocity was 30 ft/min. and dewpoint less than minus 40°F. Figures 28 through 30 indicate the number of penetrations at various depths at constant temperature. These curves follow the general decay-type curve described in WADC TR 54-120. The number of penetrations per inch of sample (Fig. 31) is roughly the same as that obtained in the commercial heats of 310 alloy. The mean depth of these fissures in the chromel ARM alloys (Fig. 32) is approximately equal to the depth obtained in the best commercial 310 alloy. The chromel D alloy shows a lesser mean depth of penetration than the best commercial 310 alloy, being on a par with inconel.

It was found in the previous year's work that little variation in intergranular penetration was encountered with variations in time from 10 to 100 hours. A 500-hour test was performed on inconel, type 310 (heat X27258), and chromel ARM heat A to determine the effect of a five-fold increase in time over the longest previous run. Figure 33 indicates the variation in number of penetrations at various depth at constant temperature. Since some of the numbers encountered are above the magnitudes of the figures in the graph, Table III lists the number of penetrations at various depths, mean depth, and total number of penetrations of the

above materials. The same data are given for the 100- and 500-hour test.

It can be seen from Table III that the 500-hour treatment on the chromel material results in a much greater number of penetrations and a greater mean depth than the 100-hour treatment. Figures 13 through 18 show the microstructure of the intergranular penetration on the 100- and 500-hour tests. In general, the 500-hour treatment on the chromel ARM heat A material resulted in a much thicker scale layer and in wider penetrations than was observed for the 100-hour test. This increased thickness of the fissures is probably due to lateral volume oxidation from the already present intergranular penetration. The 500-hour treatment also forms a much deeper and more continuous penetration.

The greater number of penetrations in the 500-hour test is probably due to the fact that some very slight penetrations in the 100-hour test may be considered surface imperfections and therefore not counted as intergranular oxidation penetration. However, after a 500-hour exposure these slight penetrations are deep enough to remove any doubt that they are penetrations. Table III also shows that longer time results in a fewer number of smaller penetrations. This is probably a result of the initial entries progressing to the medium depths. Heat X27258 (Fig. 33) of the type 310 alloy acts similarly to the chromel alloy just described; however, there is not as much thickening of the penetrations. The inconel alloy acts differently with respect to depth as can be seen from Table III and Fig. 33. The mean depth of the penetration is not altered appreciably, although the number has increased.

More metallographic work corroborated with proposed weight-gain experiments should help in further explanation of this time variation of intergranular penetration.

TABLE I  
CHEMICAL ANALYSIS OF MATERIALS, WEIGHT PERCENT

Alloy and Heat No.	Fe	N <sub>2</sub>	Mn	Si	Cr	Co	Cu	Ta	P	Ni	C	S	Mo	W	Nb
Type 310 64177	Bal.	0.1	0.42	0.55	24.03	0.01	0.13	0.01	0.018	16.93	0.13	0.008	0.033	<0.01	-
Type 310 64270	Bal.	0.06	0.50	0.43	22.30	0.01	0.10	-	0.025	19.14	0.12	0.008	0.042	<0.01	-
Type 309 + Nb	Bal.	-	2.31	0.46	22.64	-	-	-	0.012	15.39	0.080	0.008	-	-	0.82
Type 310 X11338	Bal.	-	1.53	0.83	24.44	-	0.25	-	0.029	20.08	0.080	0.029	0.14	-	-
Type 310 X27258	Bal.	-	1.58	0.75	24.80	-	0.30	-	0.025	20.81	0.070	0.008	0.15	-	-
Type 310 J 10*	Bal.	-	0.18	0.1	23.25	0.024	0.001 to 0.01	0.08	-	20.63	0.038	0.01	<0.002	0.04	<0.017
Inconel	8.25	-	-	0.19	15.72	-	-	-	-	75.18	0.05	-	-	-	-
Chromel ARM Heat A	0.39	-	1.60	1.00	19.86	-	-	-	-	77.01	0.04	-	-	-	-
Chromel ARM Heat B	0.42	-	1.53	1.06	19.83	-	-	-	-	76.36	0.1	-	-	-	-
Chromel D * Vacuum melted heat	39.76	-	0.67	1.61	21.69	-	-	-	-	35.92	0.09	-	-	-	-

TABLE II  
ANALYSES OF INTERGRANULAR OXIDES OF STAINLESS STEELS OBTAINED BY ELECTRON DIFFRACTION

Etch	Oxidizing Temperature, °F								
	1600		1700		1800		1900		2000
	Measured Depth, in.	Analysis	Measured Depth, in.	Analysis	Measured Depth, in.	Analysis	Measured Depth, in.	Analysis	Measured Depth, in.
Scale (x-ray)		Cr <sub>2</sub> O <sub>3</sub> (S) HPS (S)		Cr <sub>2</sub> O <sub>3</sub> (S) Fe <sub>2</sub> O <sub>3</sub> (S) HPS (W)		Cr <sub>2</sub> O <sub>3</sub> (S) Fe <sub>2</sub> O <sub>3</sub> (M) HPS (M)		Cr <sub>2</sub> O <sub>3</sub> (S) Fe <sub>2</sub> O <sub>3</sub> (M) HPS (M)	-
Surface	0	Sp (S) Rh (S)	0	Sp (S) Rh (S)	0	Sp (S) Rh (M)	0	Sp (S)	-
I	-	Sp (S) Rh (S)	-	Sp (S) Rh (S)	0.0002	Sp (S) Rh (M)	0.0004	Sp (S) Rh (VW)?	
II	-	M <sub>23</sub> C <sub>6</sub> ?	-	Sp (S) Rh (S)	0.0002	Sp (S) Rh (M)	0.0006		
III			-	Sp (M) Rh (M)	0.0001	Sp (W) Rh (W)	0.0007	Sp (VW) Rh (VW)	
IV					0.0004	Sp (W) Rh (W)	0.0007	Sp (VW) Rh (VW)	

HPS - High-parameter Spinel  
LPS - Low-parameter Spinel  
Sp - Spinel Phase  
Rh - Rhombohedral Phase

TABLE II (Cont'd)

Etch	Oxidizing Temperature, °F								
	1600		1700		1800		1900		2000
	Measured Depth, in.	Analysis	Measured Depth, in.	Analysis	Measured Depth, in.	Analysis	Measured Depth, in.	Analysis	Measured Depth, in.

TYPE 310 ALLOY, HEAT 64177 - Run 20

Scale (x-ray)	Cr <sub>2</sub> O <sub>3</sub>	Insuf.	X 50	X 50	X 50	-
Surface	0	Rh (S)	0	Rh (S)	0	Rh (S)
I	-	Rh (S)	-	Rh (S)	-0.0003	Rh (S)
II	-	Rh (S)	-	Rh (S)	0.0000	Rh (S)
III						Sp (VWV)?
IV						Sp (VWV)?

TABLE II (cont'd)

Etch	Oxidizing Temperature, °F								
	1600		1700		1800		1900		2000
	Measured Depth, in.	Analysis	Measured Depth, in.	Analysis	Measured Depth, in.	Analysis	Measured Depth, in.	Analysis	Measured Depth, in.

TYPE 310 ALLOY, HEAT 64270 - Run 20

Scale (x-ray)	X 50		Fe <sub>2</sub> O <sub>3</sub> LPS (M)	X 50 (S) LPS (W)	X 50 (S) Re <sub>2</sub> O <sub>3</sub> (W)?				
Surface	0	Rh (S)	0	0	0	Rh (S) Sp (VW)?	0	Rh (S) Sp (VW)	-
I			-0.0002	Rh (S)	0.0000	Rh (S)	0.0000	Rh (S) Sp (VW)	
II			0.0000	Rh (W)	0.0004	Rh (S)	0.0001	Rh (S) Sp (VW)?	
III			-0.0001	No Pattern	0.0006	Rh (M)	0.0003	Rh (M) Sp (VW)?	
IV					0.0007	Metal	0.0001	Metal	

TABLE II (cont'd)

Etch	Oxidizing Temperature, °F												
	1600		1700		1800		1900		2000				
	Measured Depth, in.	Analysis	Measured Depth, in.	Analysis	Measured Depth, in.	Analysis	Measured Depth, in.	Analysis	Measured Depth, in.	Analysis	Measured Depth, in.	Analysis	
TYPE 310 ALLOY, HEAT X11306													
Scale (x-ray)		Fe <sub>2</sub> O <sub>3</sub> (S) HPS (M)											
Surface	0	Sp (S) Rh (M)	0	Sp (S) Rh (M)	0	Sp (S) Rh (W)	0	Sp (S)	0	Sp (S)	0	Sp (S) Rh (VW)?	X 75 (S) LPS (S) HPS (M)
I	0.0002	Sp (S) Rh (VW)?	0.0000	Sp (S) Rh (M)	0.0000	Contam.	0.0003	Sp (S)	0.0002	Sp (S)	0.0002	Sp (S) Rh (VW)?	Sp (S) Rh (VW)?
II	0.0001	Sp (S)	0.0000	Sp (S) Rh (M)	0.0000	Sp (M) Rh (VW)?	0.0003	Sp (S)	-0.0001	Sp (S)	-0.0001	Sp (W) Rh (VW)?	Sp (W) Rh (VW)?
III	0.0001	Sp (S)	0.0001	Sp (M) Rh (M)	0.0002	Sp (S) Rh (M)	0.0004	Sp (M) Rh (M)	-0.0002	Sp (M) Rh (M)	-0.0002	Sp (VW)? Rh (VW)	Sp (VW)? Rh (VW)
IV	0.0002	Metal	0.0001	Sp (M) Rh (M)	0.0000		0.0004	Sp (W) Rh (W)	-0.0003	Sp (W) Rh (W)	-0.0003	Sp (VVW) Rh (VW)	Sp (VVW) Rh (VW)
V			0.0001	Sp (VW) Rh (VW)	0.0000	Sp (M) Rh (W)	0.0002	Sp (M) Rh (M)		Sp (M) Rh (M)			
VI				Sp (W) Rh (VW)?	0.0001	Sp (W) Rh (VW)?	0.0000	Sp (M) Rh (W)		Sp (M) Rh (W)			
VII				Sp (W) Rh (VW)?	0.0001	Sp (W) Rh (VW)?	0.0003	Sp (W) Rh (W)		Sp (W) Rh (W)			
VIII				Sp (VW) Rh (VW)?	0.0001	Sp (VW) Rh (VW)?	0.0007	Sp (VW) Rh (VW)?		Sp (VW) Rh (VW)			

TABLE II (cont'd)

Etch	Oxidizing Temperature, °F									
	1600		1700		1800		1900		2000	
	Measured Depth, in.	Analysis	Measured Depth, in.	Analysis	Measured Depth, in.	Analysis	Measured Depth, in.	Analysis	Measured Depth, in.	Analysis
TYPE 310 ALLOY, HEAT X11358										
Scale (x-ray)		Cr <sub>2</sub> O <sub>3</sub> (S) HPS (S)		Cr <sub>2</sub> O <sub>3</sub> (S) HPS (S) LPS (W)		Cr <sub>2</sub> O <sub>3</sub> (S) HPS (S) LPS (W)		X 25 (S) LPS (M)		X 25 (S) LPS (M)
Surface	0	Sp (S) Rh (S)	0	Sp (S) Rh (S)	0	Sp (S) Rh (W)	0	Sp (S)	0	Sp (S) Rh (VW)
I	0.0001	Sp (S) Rh (S)	0.0002	Sp (S) Rh (S)	0.0001	Contam.	0.0002	Sp (S)	0.0003	Sp (S) Rh (W)
II	0.0001	Sp (S) Rh (S)	0.0002	Sp (S) Rh (S)	0.0001	No Pattern	0.0002	Sp (S) Rh (S)	0.0003	Rh (M)
III	0.0001	Sp (W) Rh (M)	0.0003	Sp (M) Rh (VW)?	0.0004	No Pattern	0.0002	Sp (M) Rh (M)	0.0005	Sp (M) Rh (M)
IV	0.0001	No Pattern	0.0002	Sp (W) Rh (VW)?			0.0004	Sp (S) Rh (S)	0.0004	Sp (M) Rh (M)
V							0.0002	Sp (M) Rh (M)	0.0004	Sp (VW) Rh (VW)
VI							0.0002	Sp (M) Rh (W)	0.0004	Sp (VW) Rh (VW)?
VII							0.0002	Sp (M) Rh (W)		
VIII							0.0002	Sp (VW) Rh (VW)?		



TABLE II (cont'd)

Etch	Oxidizing Temperature, °F									
	1600		1700		1800		1900		2000	
	Measured Depth, in.	Analysis	Measured Depth, in.	Analysis	Measured Depth, in.	Analysis	Measured Depth, in.	Analysis	Measured Depth, in.	Analysis
Scale (x-ray)		Cr <sub>2</sub> O <sub>3</sub> (S) HPS (S)	X 75 (S) HPS (S) LPS (W)	Cr <sub>2</sub> O <sub>3</sub> (S) HPS (S) LPS (W)?	X 50 (S) HPS (S)	Cr <sub>2</sub> O <sub>3</sub> (S) HPS (S)				
Surface	0	Sp (S) Rh (S)	0	Sp (S) Rh (M)	0	Sp (S) Rh (W)	0	Sp (S) Rh (W)?	0	Sp (S) Rh (W)
I	0.0000	Sp (S) Rh (M)	0.0002	Sp (S) Rh (M)	-0.0001	Sp (S) Rh (W)?	0.0001	Sp (S)	-0.0001	Sp (S) Rh (W)
II	0.0000	Sp (S) Rh (S)	0.0005	Sp (S) Rh (M)	0.0002	Sp (M) Rh (W)	0.0003	Sp (S) Rh (W)	0.0001	Sp (M) Rh (M)
III	0.0001	No Pattern	0.0006	Sp (S) Rh (M)	0.0005	Sp (S) Rh (M)	0.0006	Sp (S) Rh (S)	0.0000	Sp (VW) Rh (W)
IV	0.0002	No Pattern	0.0008	No Pattern	0.0005	Sp (S) Rh (M)	0.0005	Contam.	0.0001	Sp (VW) Rh (VW)
V			0.0007	No Pattern	0.0003	Sp (M) Rh (W)	0.0005	Sp (S) Rh (S)	0.0000	Sp (VW) Rh (VW)
VI			0.0004	Sp (W) Rh (VW)?	0.0004	Sp (W) Rh (VW)?	0.0007	No Pattern	-0.0001	Sp (VW) Rh (VW)?
VII			0.0005	No Pattern						

TYPE 310 ALLOY, HEAT X27258

TABLE III

PENETRATION DISTRIBUTION

Alloy and Heat No.	Time in Hrs	Run No.	Penetration Depth in 0.001 inch							Total No.	Mean Depth in 0.001"
			0 to 0.64	0.64 to 1.28	1.28 to 1.92	1.92 to 2.56	2.56 to 3.2	3.2 to 3.74	3.74 up		
Chromel ARM Heat A	100	34	1049*	434	24.8	1.8				1510	0.524
Chromel ARM Heat A	500	36	438	1342	473	127	41	16	3.5	2440	1.078
Type 310 X27258	100	16	510	418	27					1015	0.623
Type 310 X27258	500	36	673	951	261	99	45	18		2047	0.948
Inconel	100	30C	896	247	7.1	7				1150	0.463
Inconel	500	36	1642	348	49					2046	0.464

\*The numbers in these columns represent number of penetrations per inch.

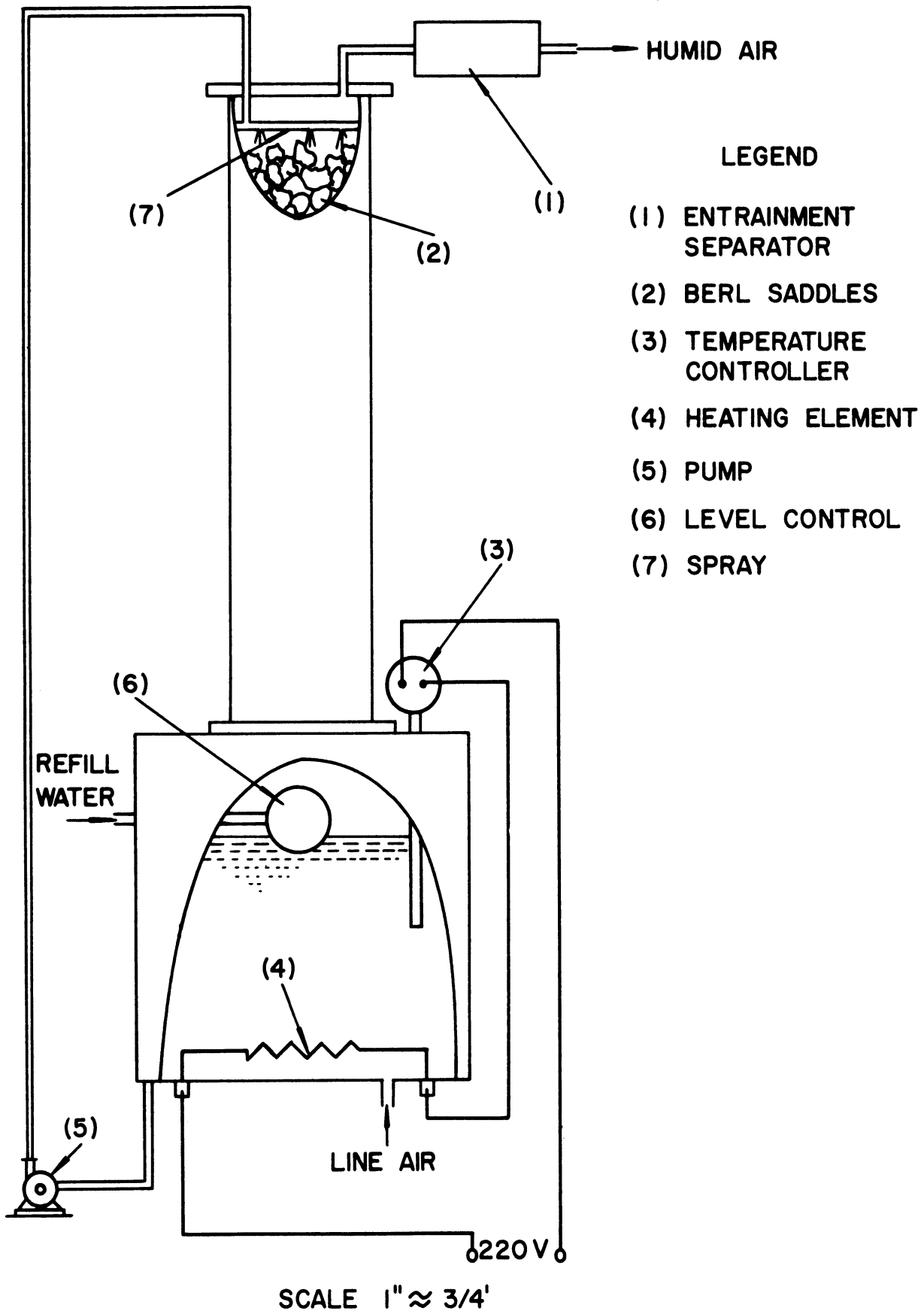
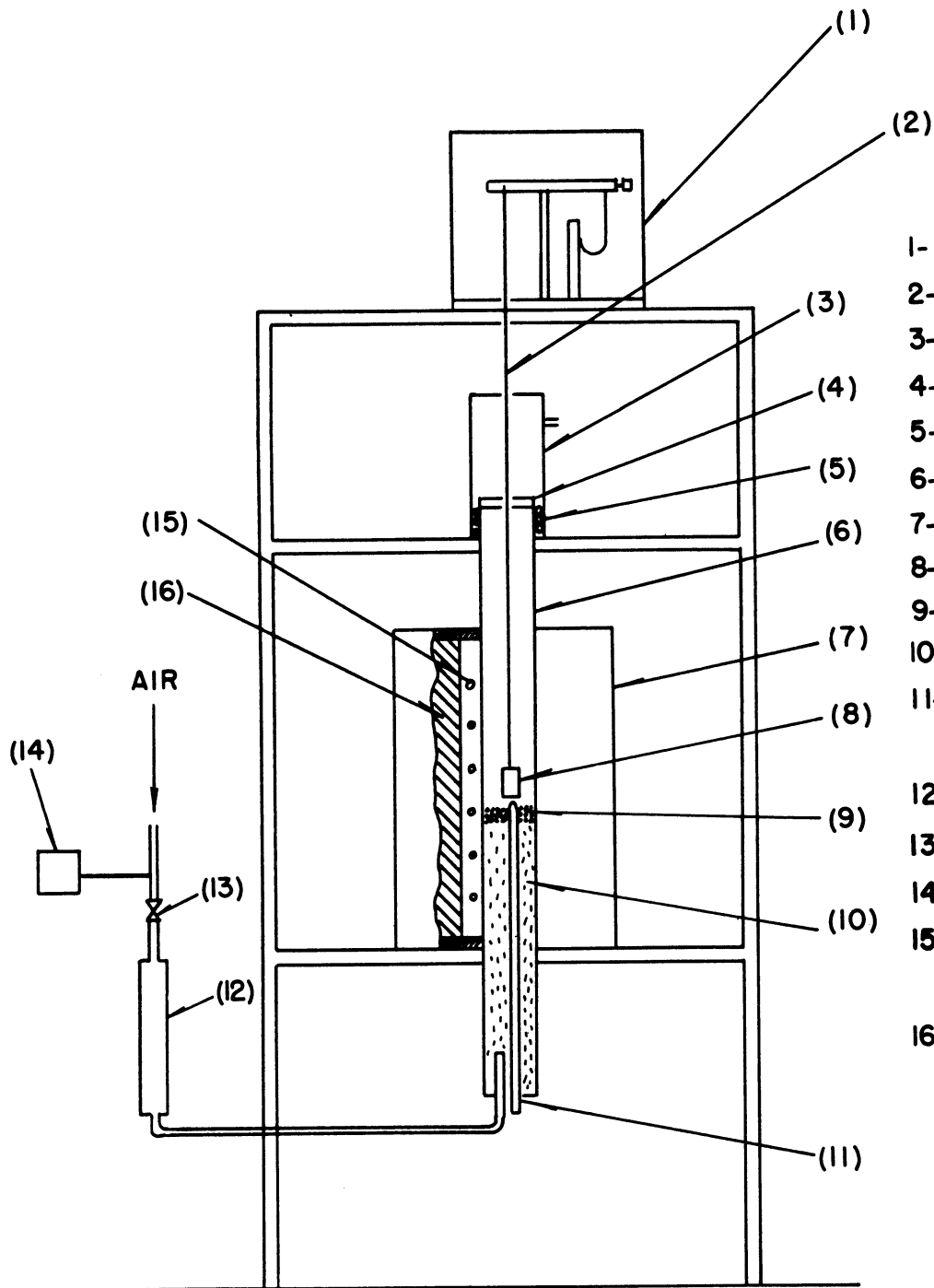


FIG.1- SCHEMATIC DRAWING OF HUMIDIFIER UNIT



**LEGEND**

- 1- CHAINOMATIC BALANCE
- 2- PLATINUM WIRE
- 3- PYREX GLASS
- 4- TRANSITE BAFFLE
- 5- COOLING COILS
- 6- SILIMANITE TUBE
- 7- FURNACE
- 8- SPECIMEN
- 9- PORCELAIN BEADS
- 10- BROKEN CERAMIC
- 11- INDICATING THERMO-  
COUPLE
- 12- ROTAMETER
- 13- VALVE
- 14- DEW PT. INDICATOR
- 15- CHROMEL COILS  
EMBEDDED IN ALUNDUM
- 16- VERMICULITE

**FIG. 2 - WEIGHT GAIN UNIT**

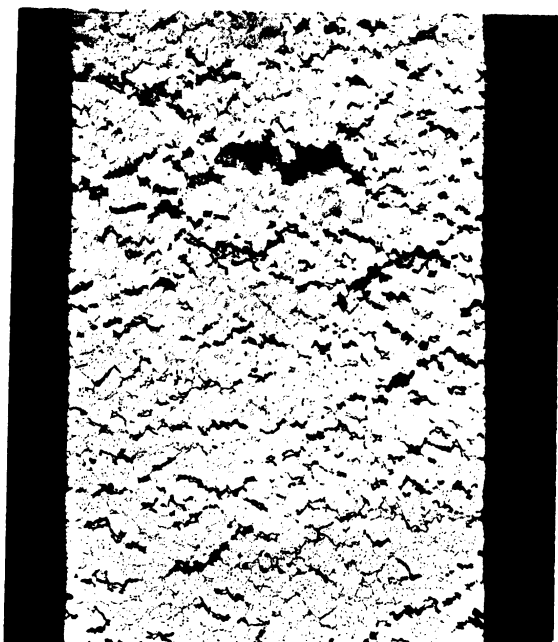


Fig. 3. Prerupture fissure and X-phase particles. Chromel ARM alloy. Heat A. 1800°F, 100 hours. Stress - 2000 psi. 50X. Cross section, unetched, oblique light.

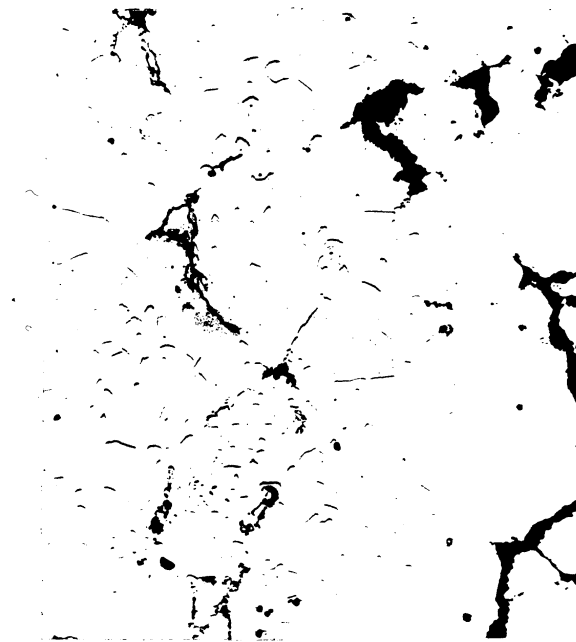


Fig. 4. Prerupture fissures and X-phase particles. Chromel ARM alloy. Heat A. 1800°F, 100 hours. Stress - 2000 psi. 750X. Cross section, unetched, oblique light.



Fig. 5. Typical electron diffraction pattern of rhombohedral phase.

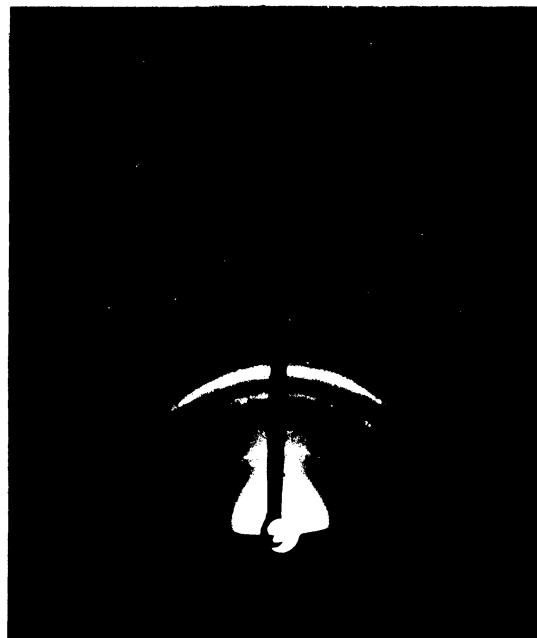


Fig. 6. Typical electron diffraction pattern of spinel phase. Some rhombohedral phase also present.

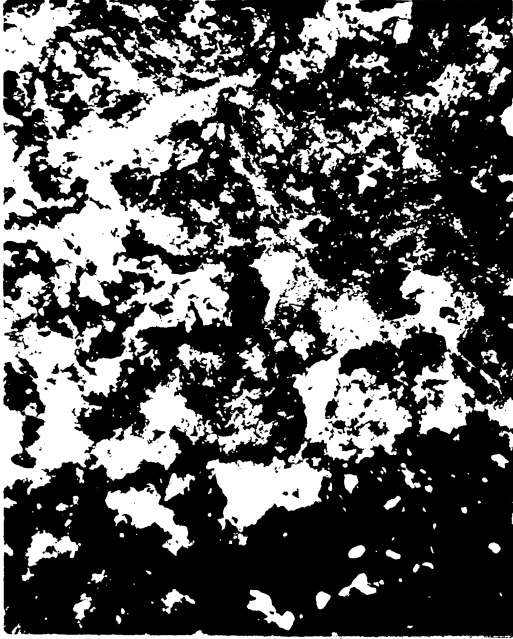


Fig. 7. Metallographic appearance of typical oxidized specimen surface. Unetched. 250X, oblique light.

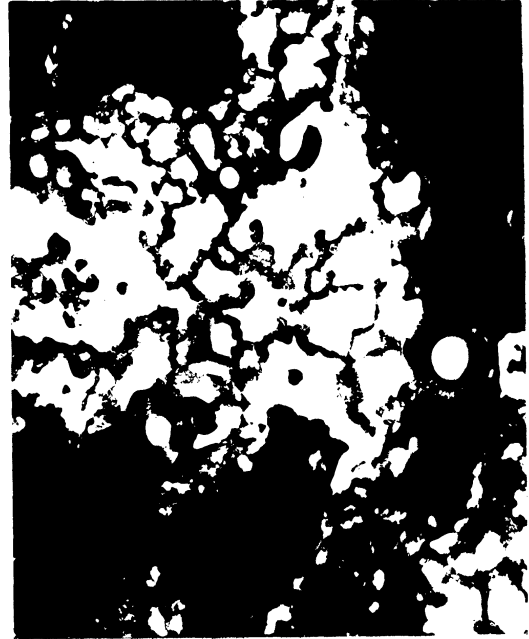


Fig. 8. Metallographic appearance of typical oxidized specimen surface after 4 min. Electrolytically etch in 90% glacial acetic acid - 10% perchloric acid. Removed 0.0004 in. 250X. Oblique light.



Fig. 9. Metallographic appearance of typical oxidized specimen surface after 10 min. Electrolytically etch in 90% glacial acetic acid - 10% perchloric acid. Removed 0.0004 in. 250X. Oblique light.



Fig. 10. Metallographic appearance of typical oxidized specimen surface after 12 min. Electrolytically etch in 90% glacial acetic acid - 10% perchloric acid. Removed 0.0011 in. 250X. Oblique light.



Fig. 11. Chromel ARM alloy. Heat A.  
1900°F, 100 hours. Stress - 250 psi.  
750X. Cross section, unetched.



Fig. 12. Chromel ARM alloy. Heat A.  
1900°F, 100 hours. Stress - 500 psi.  
750X. Cross section, unetched.



Fig. 13. Inconel alloy. 1900°F, 100  
hours. Air velocity - 30 ft/min.  
750X. Cross section, unetched.



Fig. 14. Inconel alloy, 1900°F, 500  
hours. Air velocity - 30 ft/min.  
750X. Cross section, unetched.



Fig. 15. Chromel ARM alloy. Heat A. 1900°F, 100 hours. Air velocity - 30 ft/min. 750X. Cross section, unetched.



Fig. 16. Chromel ARM alloy. Heat A. 1900°F, 500 hours. Air velocity - 30 ft/min. 750X. Cross section, unetched.



Fig. 17. Type 310 alloy. Heat X27258. 1900°F, 100 hours. Air velocity - 30 ft/min. 750X. Cross section, unetched.



Fig. 18. Type 310 alloy. Heat X27258. 1900°F, 500 hours. Air velocity - 30 ft/min. 750X. Cross section, unetched.



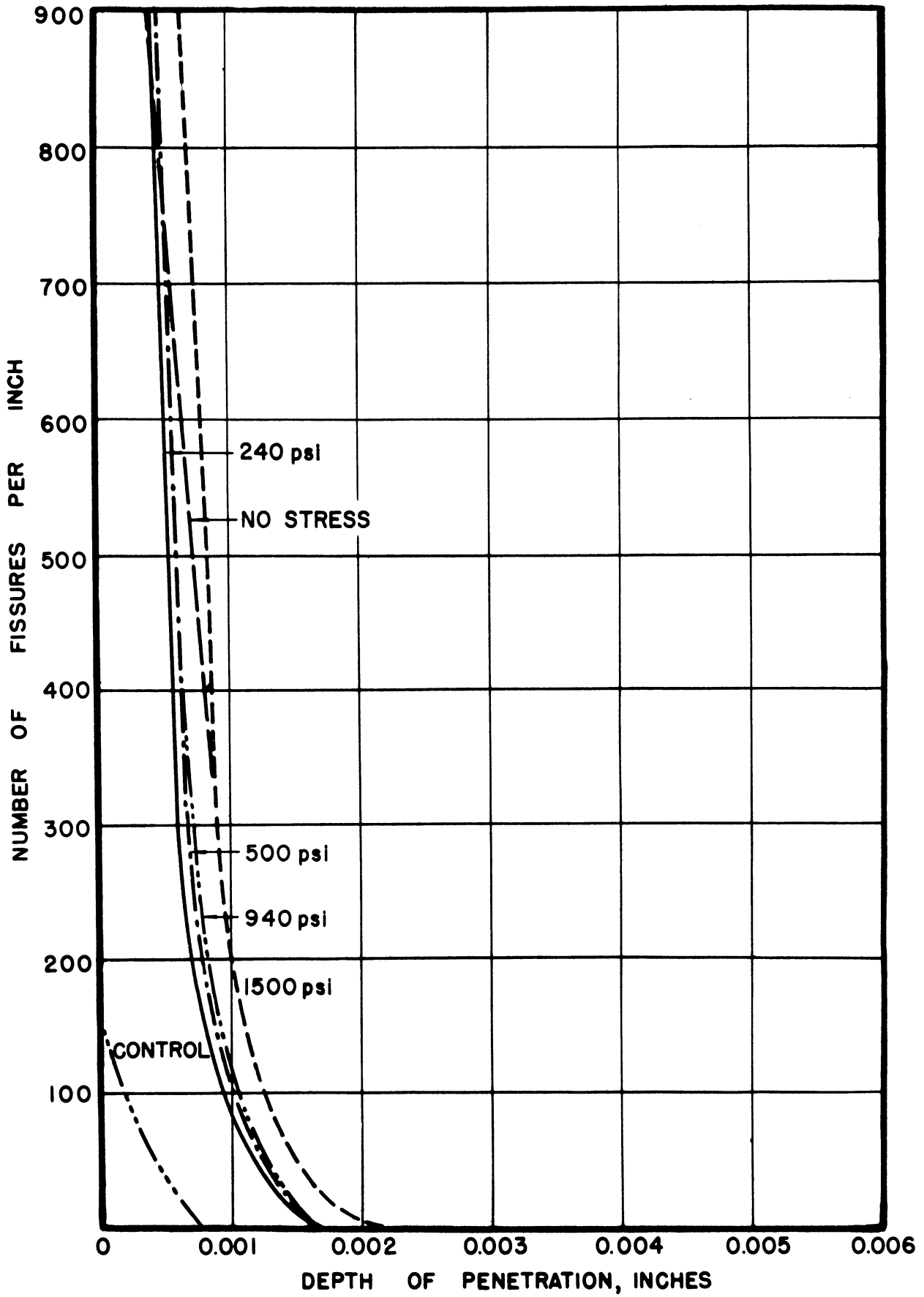


FIG.19 - PENETRATION VS. DEPTH BELOW SURFACE.  
 CHROMEL ARM HEAT A, 1800°F. 100 HRS.

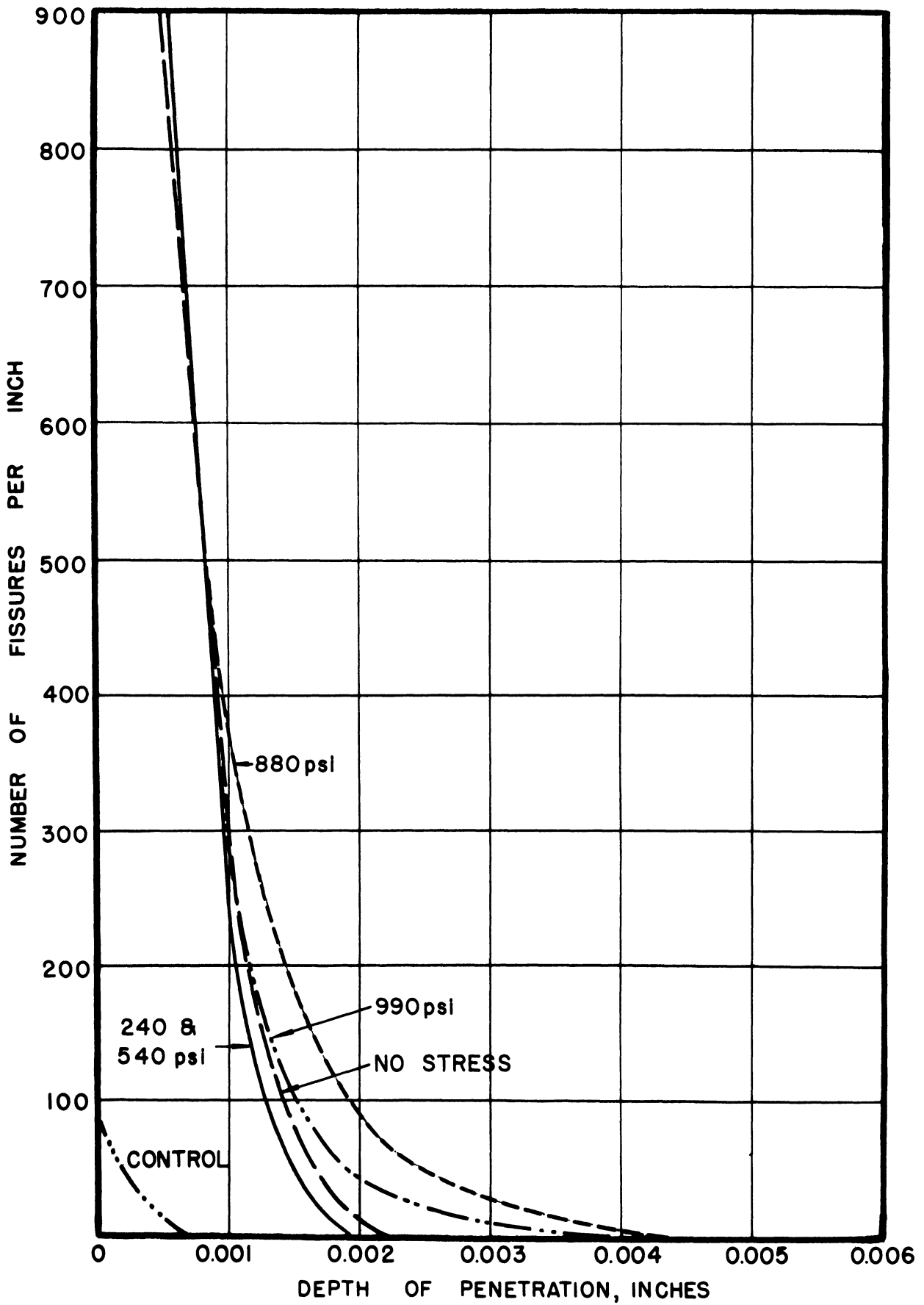


FIG.20-PENETRATION VS. DEPTH BELOW SURFACE.  
 CHROMEL ARM HEAT A , 1900°F. 100 HRS .

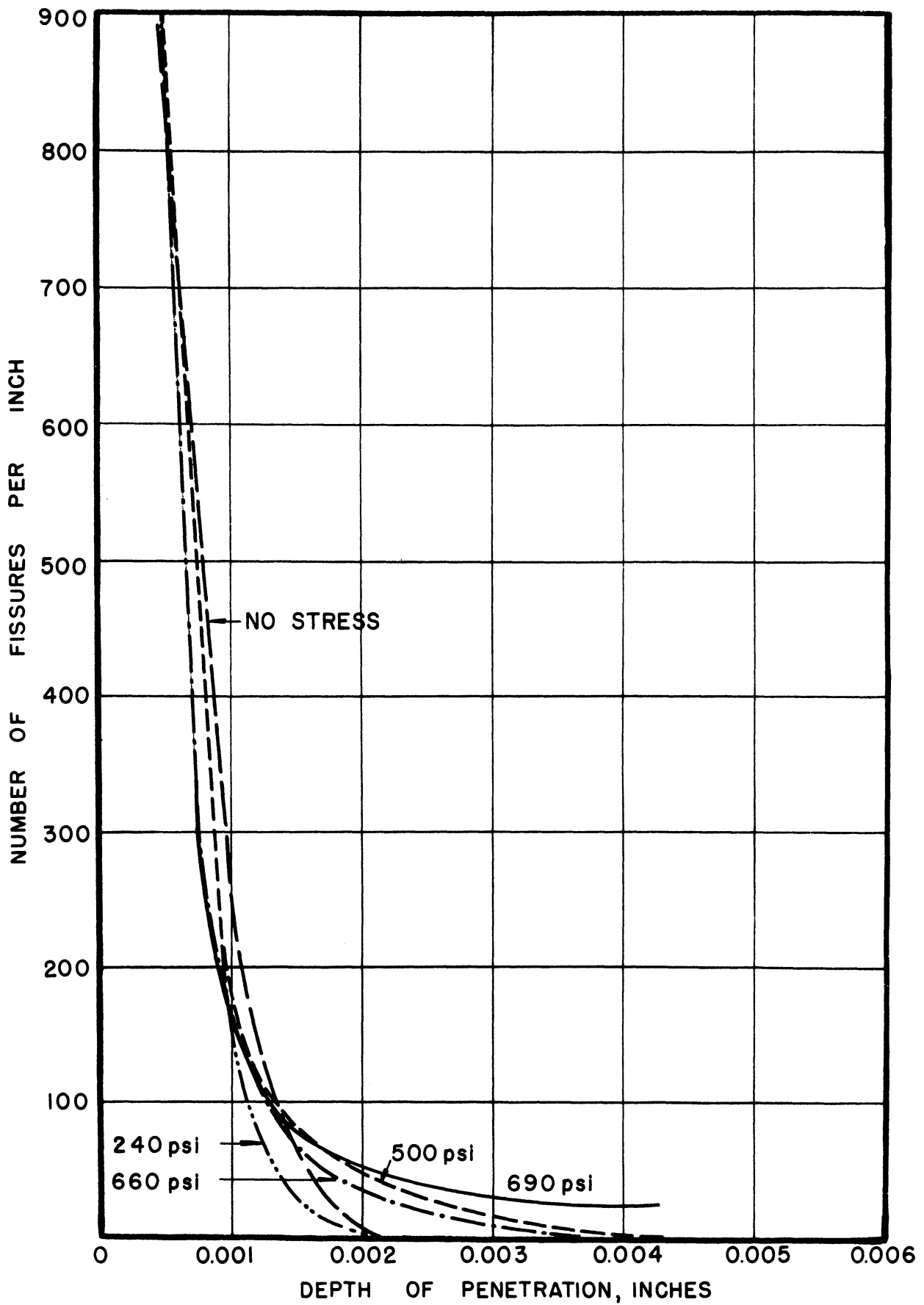


FIG.21 - PENETRATION VS. DEPTH BELOW SURFACE.  
 CHROMEL ARM HEAT A , 2000°F. 100 HRS .

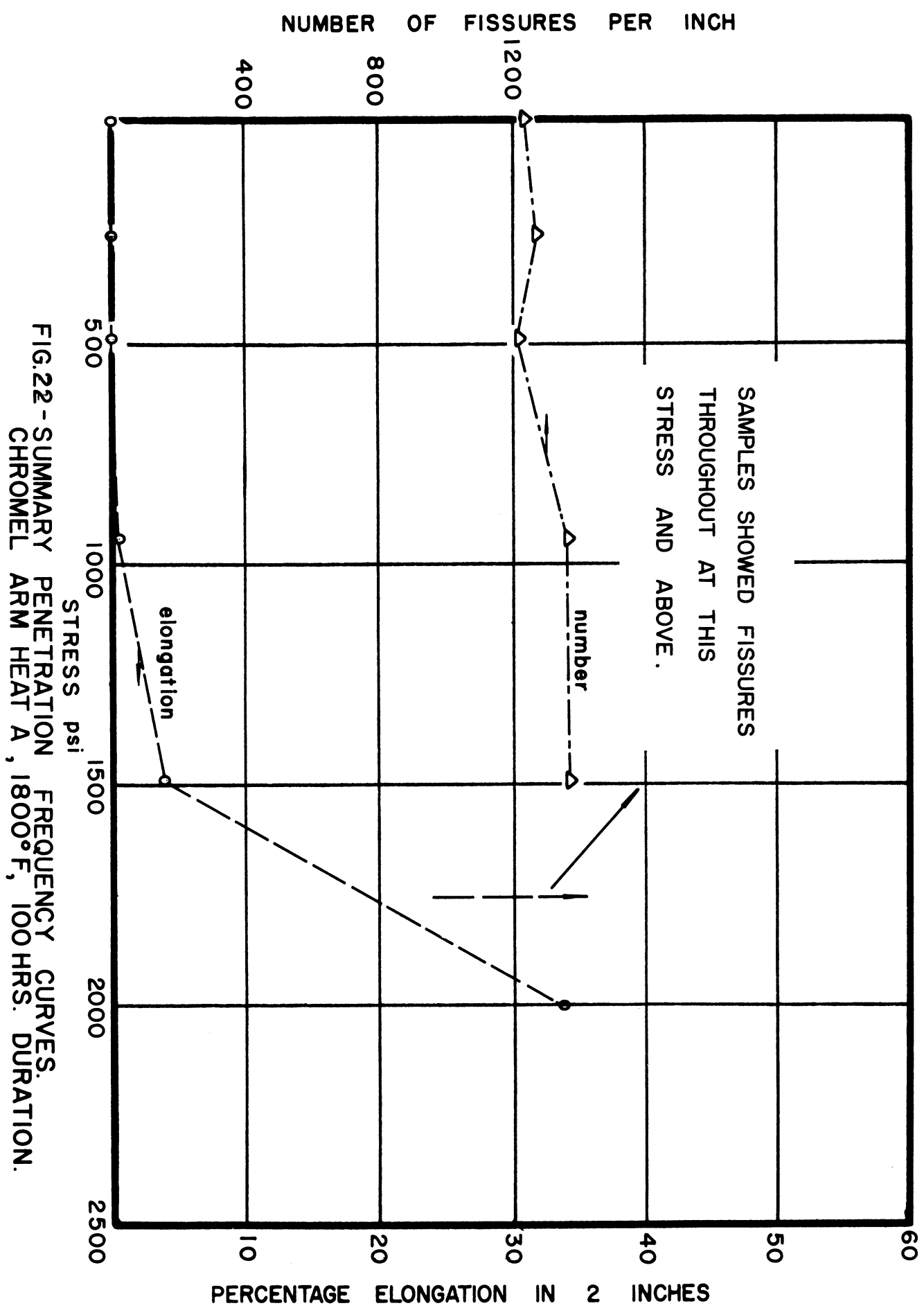


FIG.22 - SUMMARY PENETRATION FREQUENCY CURVES.  
 CHROMEL ARM HEAT A, 1800°F, 100 HRS. DURATION.

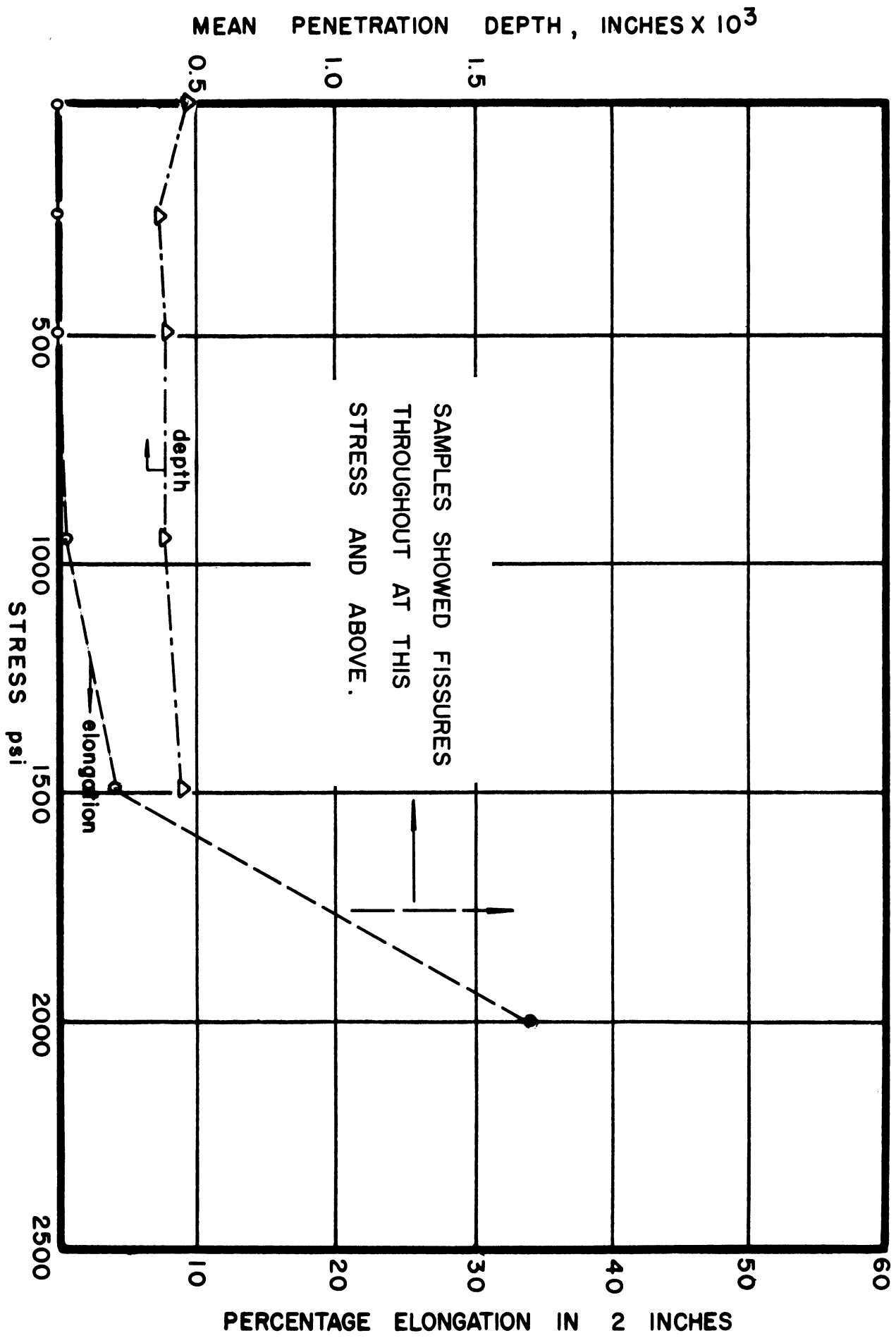


FIG23-SUMMARY PENETRATION DEPTH CURVES.  
 CHROMEL ARM HEAT A, 1800°F, 100HRS. DURATION.

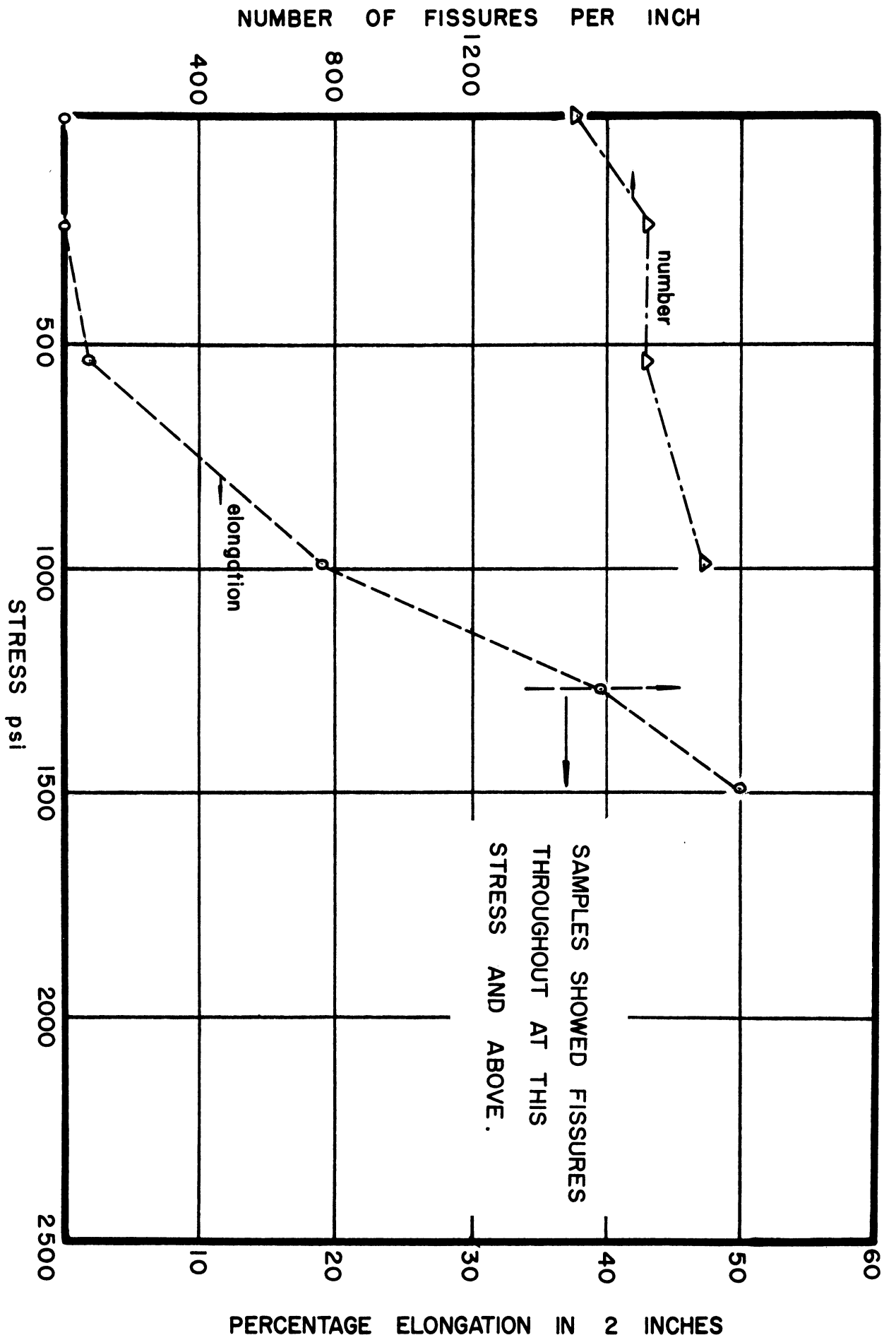


FIG.24-SUMMARY PENETRATION FREQUENCY CURVES.  
 CHROMEL ARM HEAT A, 1900°F. 100 HRS DURATION.

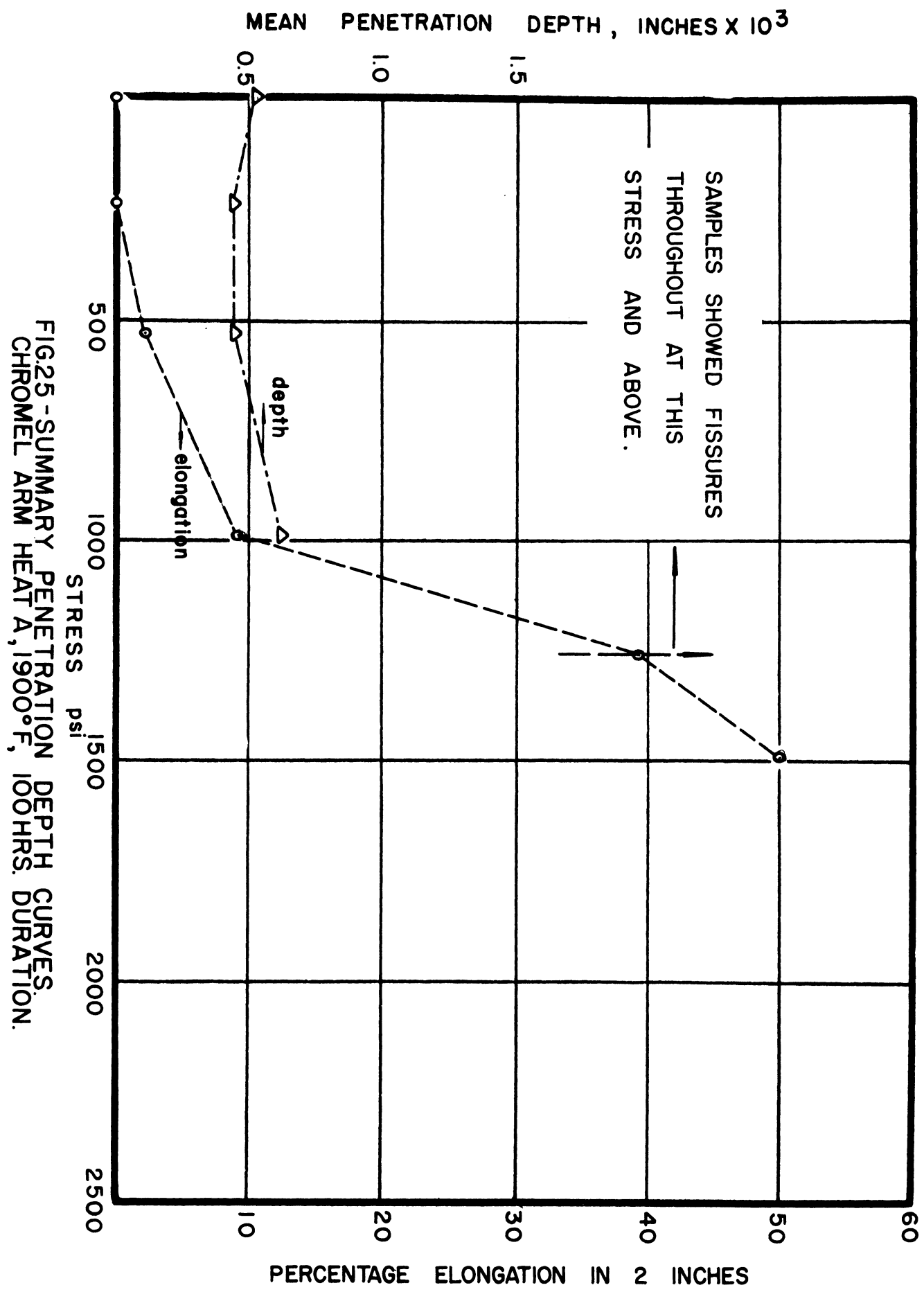


FIG25 - SUMMARY PENETRATION DEPTH CURVES.  
 CHROMEL ARM HEAT A, 1900°F, 100 HRS. DURATION.

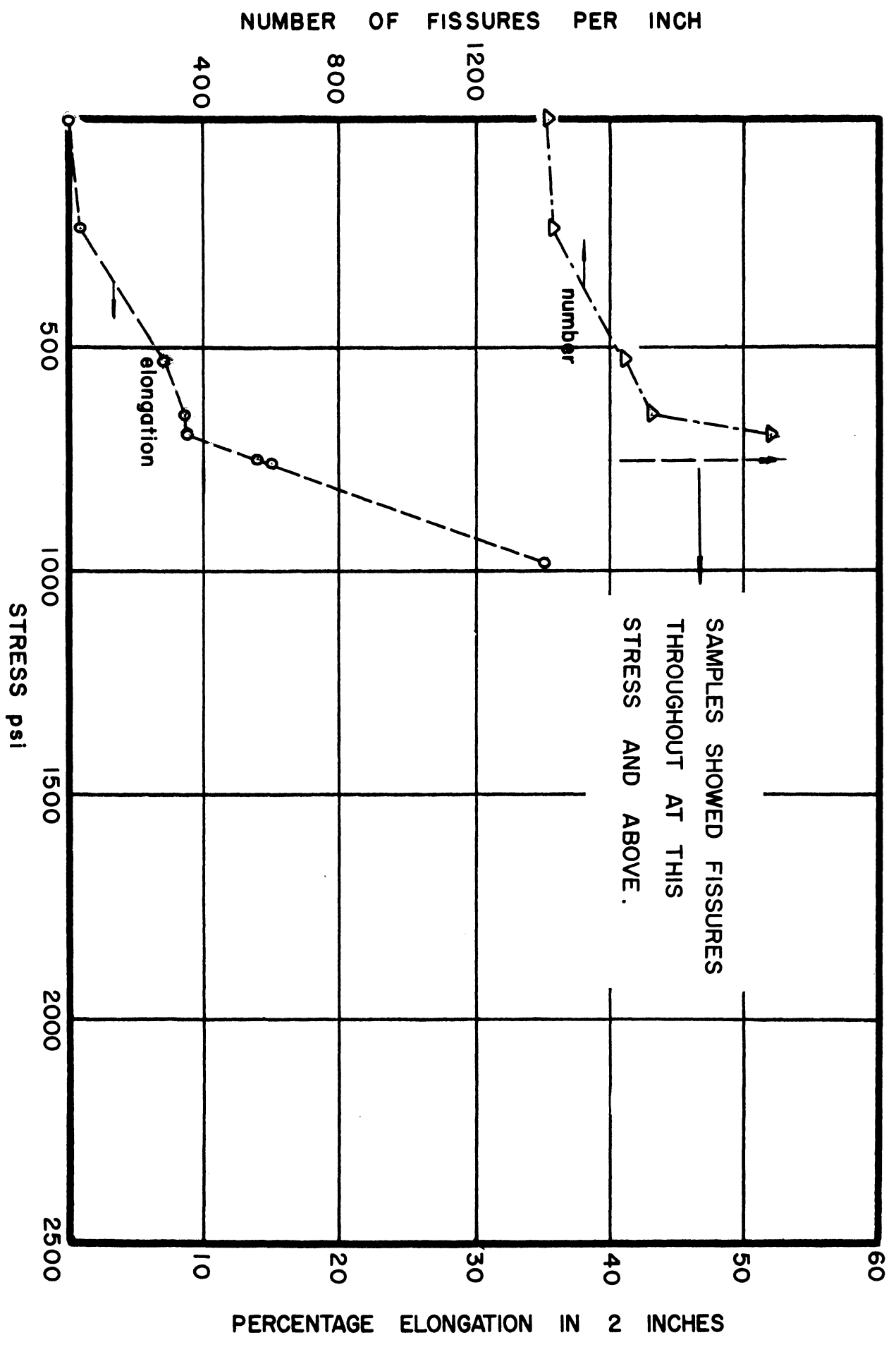


FIG.26 - SUMMARY PENETRATION FREQUENCY CURVES.  
 CHROMEL ARM HEAT A, 2000°F. 100 HRS DURATION.



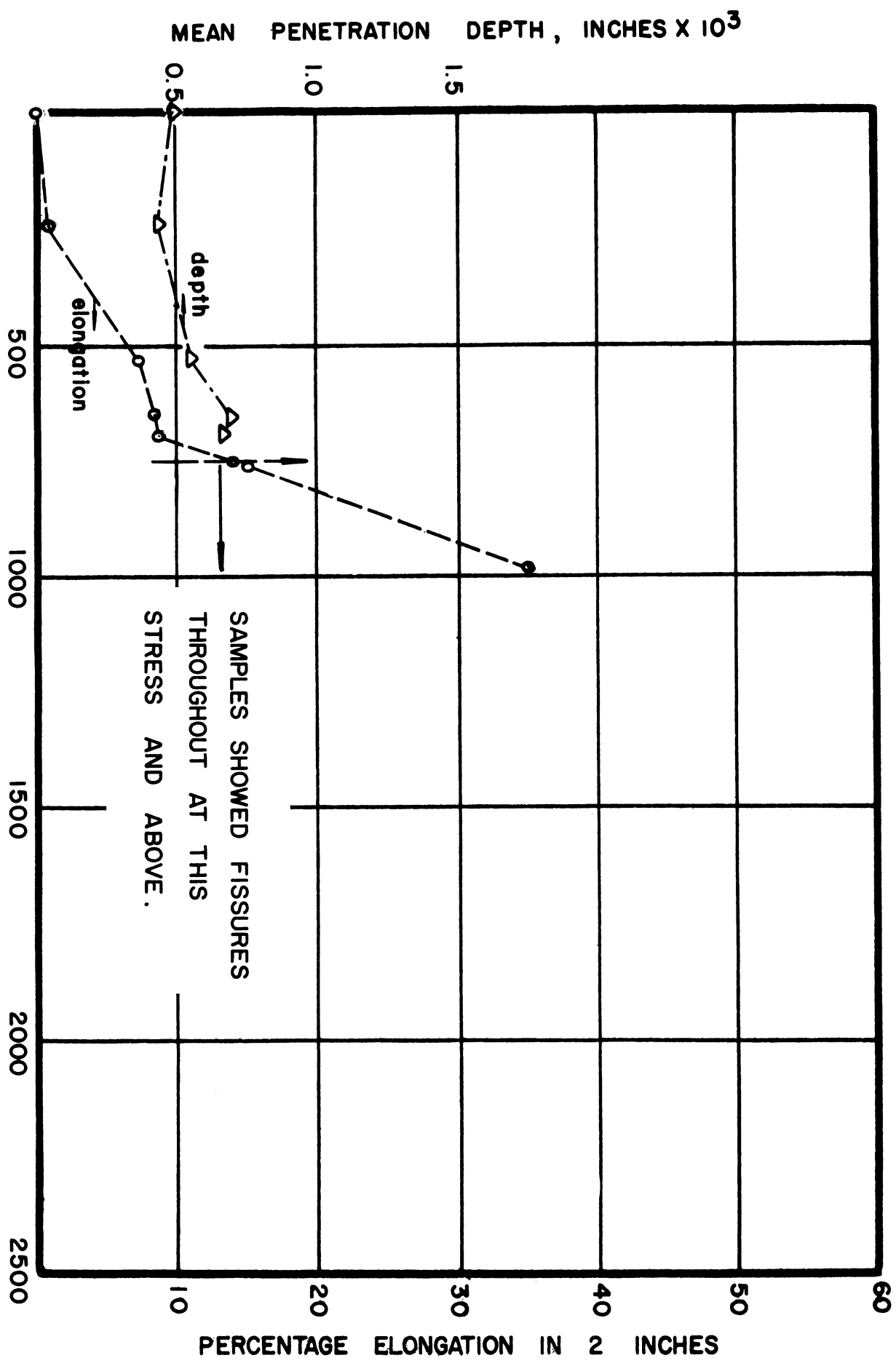


FIG.27-SUMMARY PENETRATION DEPTH CURVES.  
 CHROMEL ARM HEAT A, 2000°F. 100 HRS DURATION.

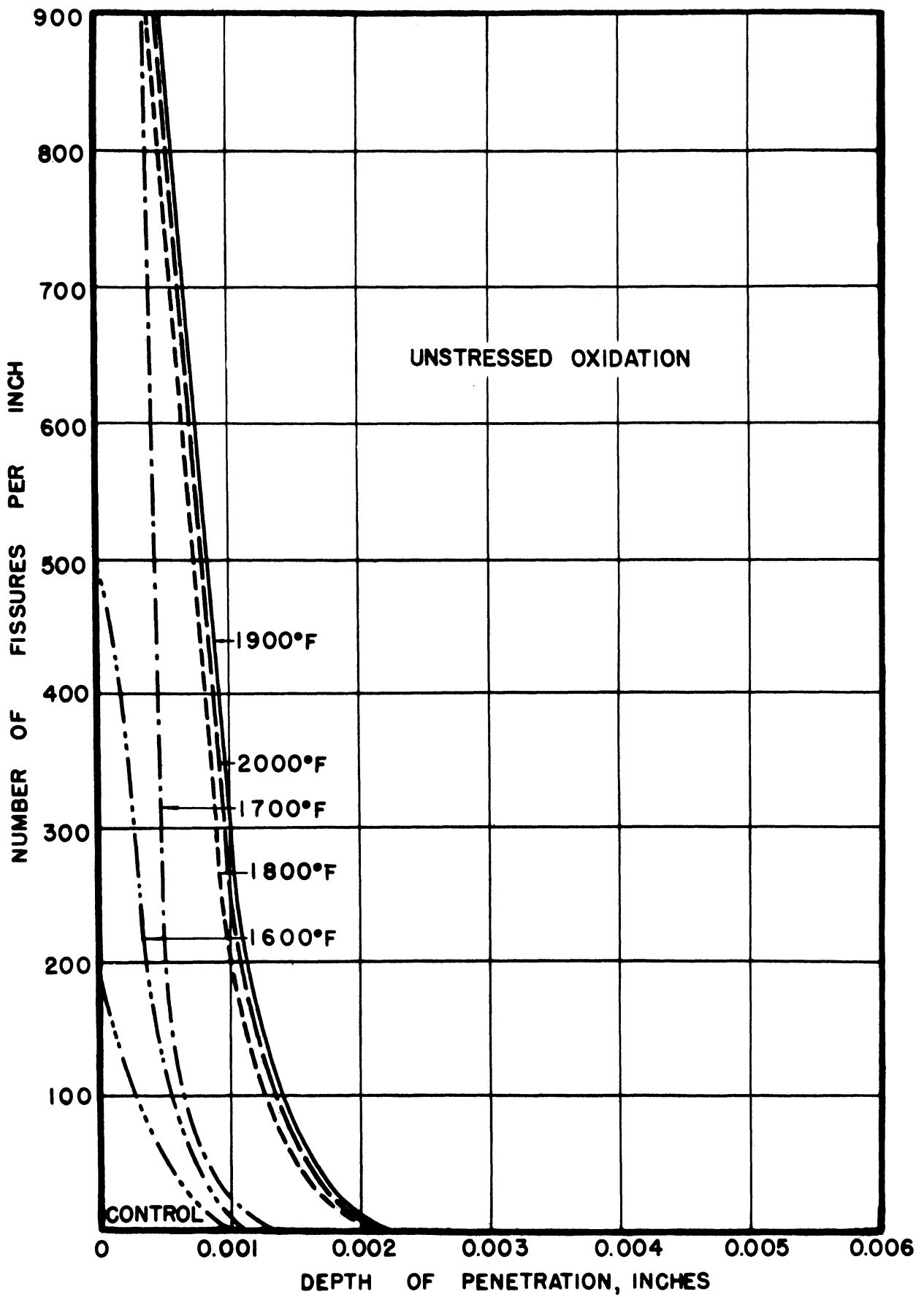


FIG.28 - PENETRATION VS. DEPTH BELOW SURFACE.  
 CHROMEL ARM HEAT A , 100 HRS.

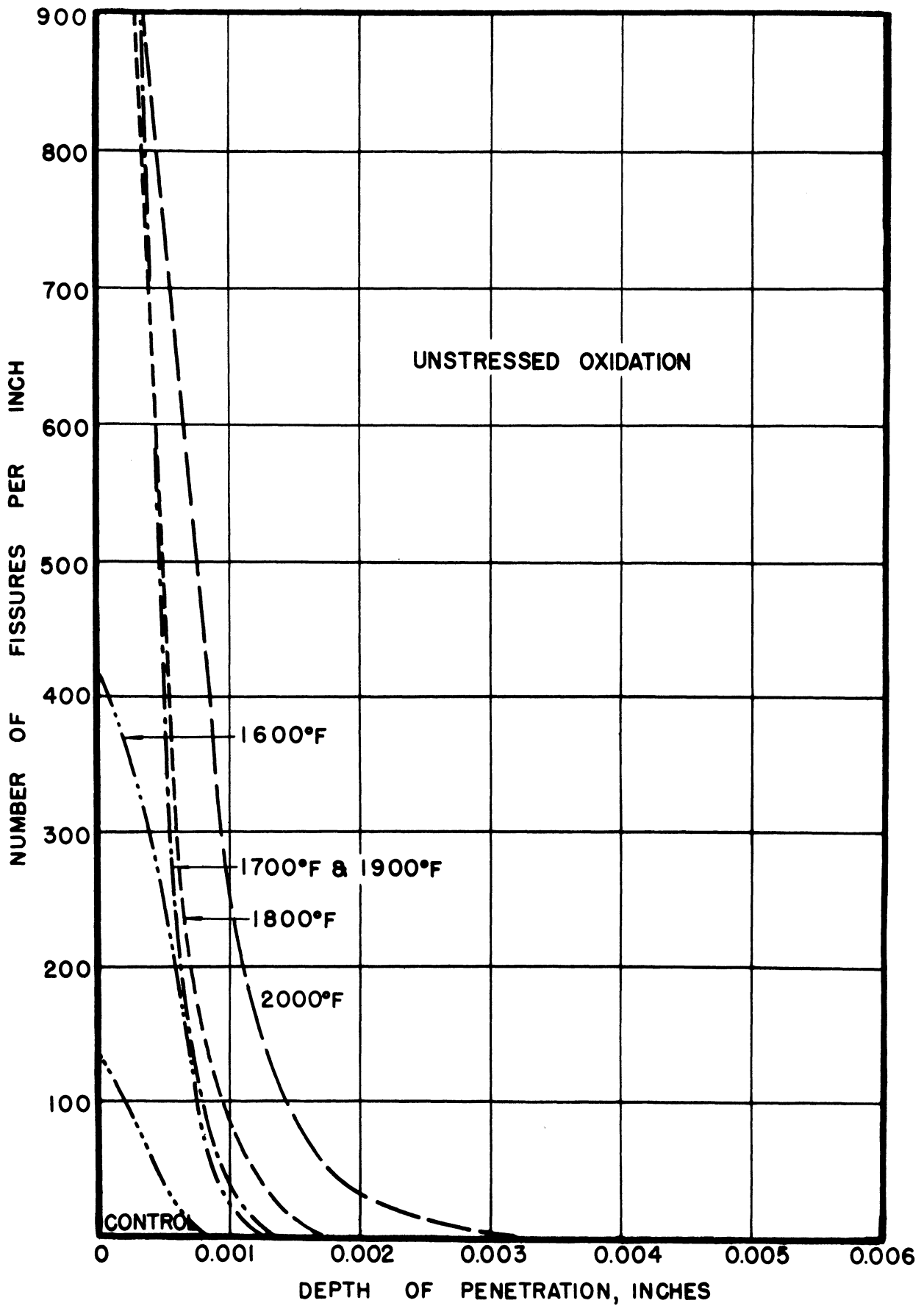


FIG.29-PENETRATION VS DEPTH BELOW SURFACE.  
 CHROMEL ARM HEAT B,RUNS 34 & 34'. 100 HRS.

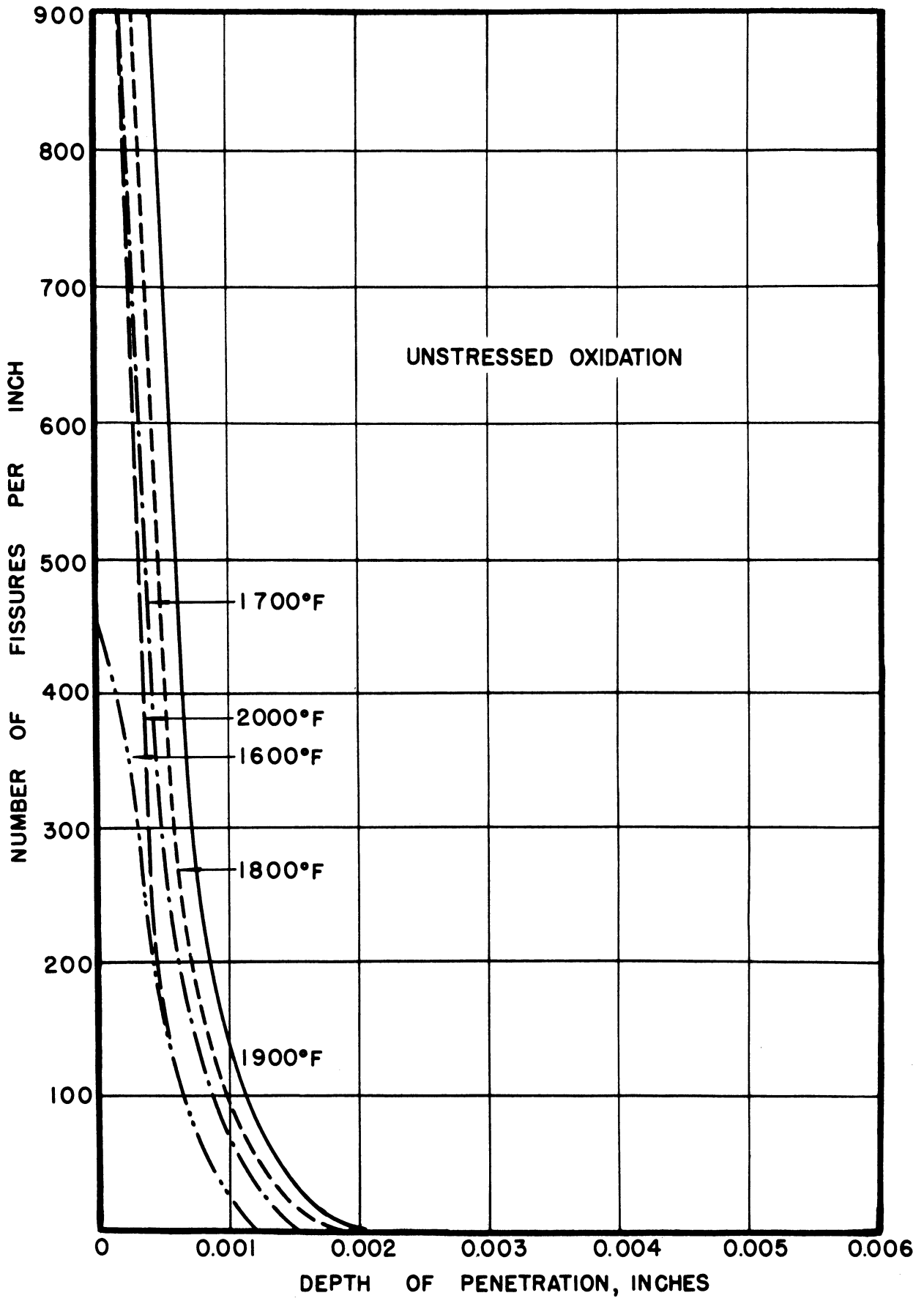


FIG.30 - PENETRATION VS. DEPTH BELOW SURFACE.  
 CHROMEL D ALLOY , 100 HRS.

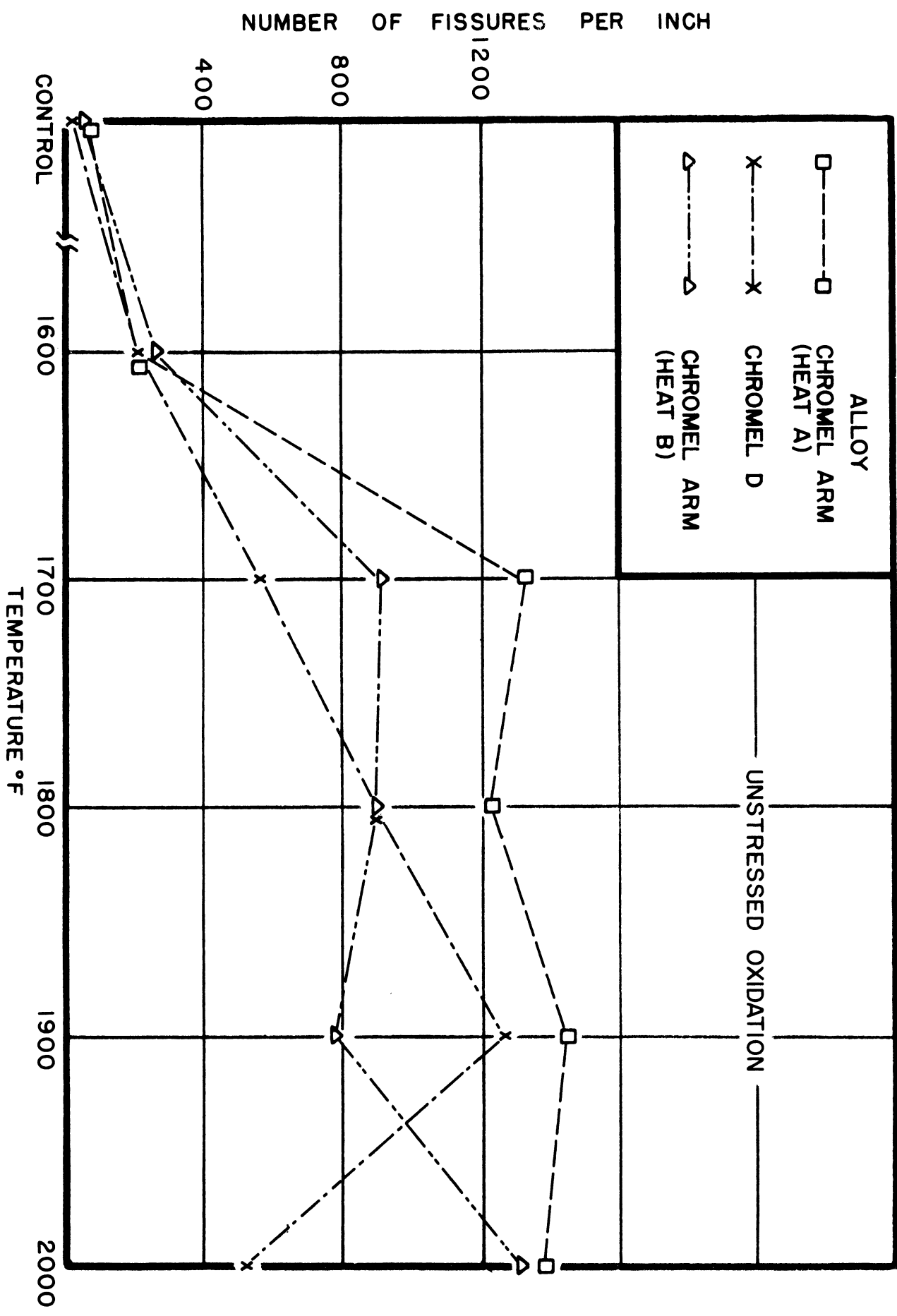


FIG. 31 - SUMMARY PENETRATION FREQUENCY CURVES  
 CHROMEL ALLOYS. 100 HRS DURATION.

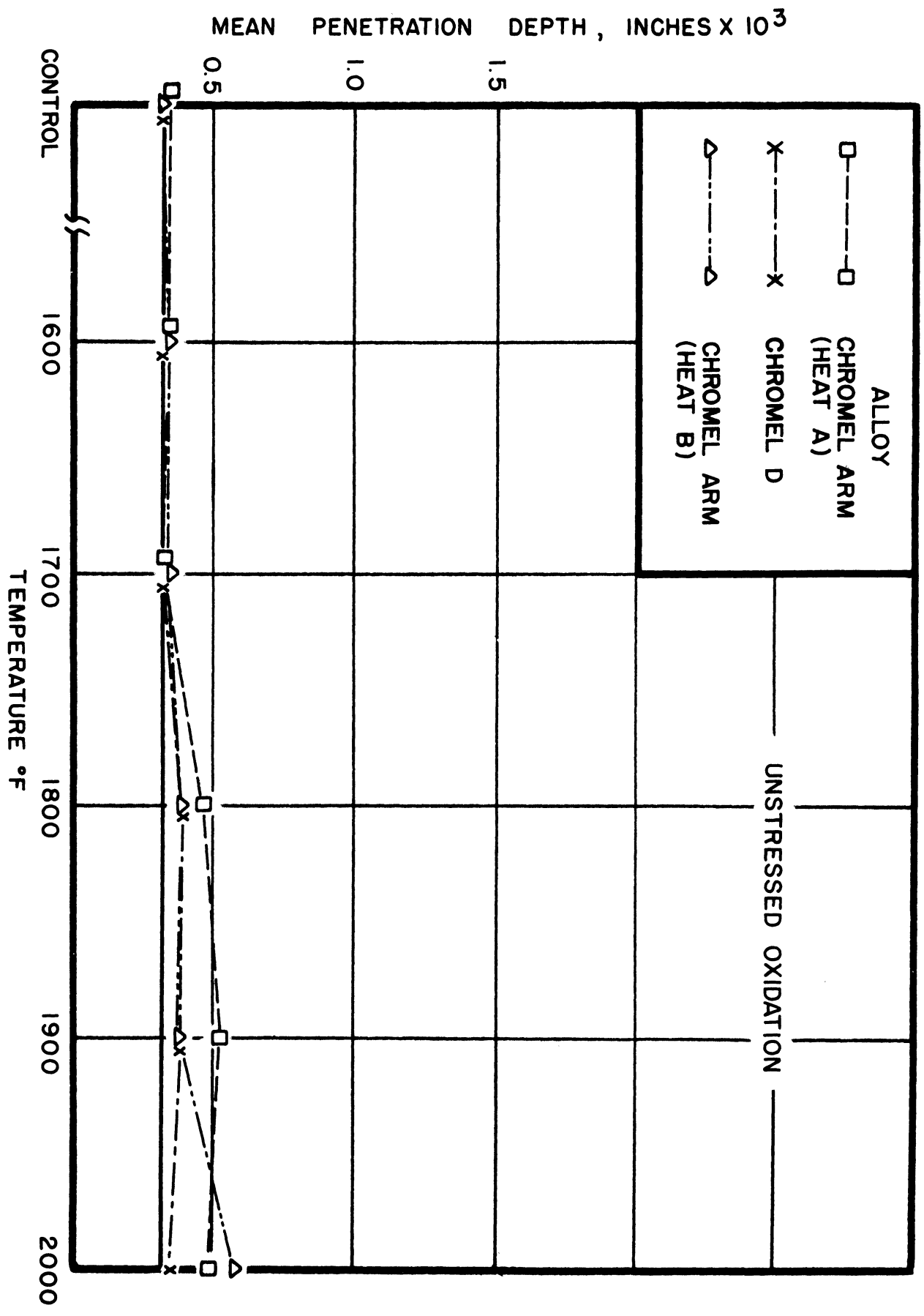


FIG. 32 - SUMMARY PENETRATION DEPTH CURVES.  
 CHROMEL ALLOYS, 100 HRS DURATION.

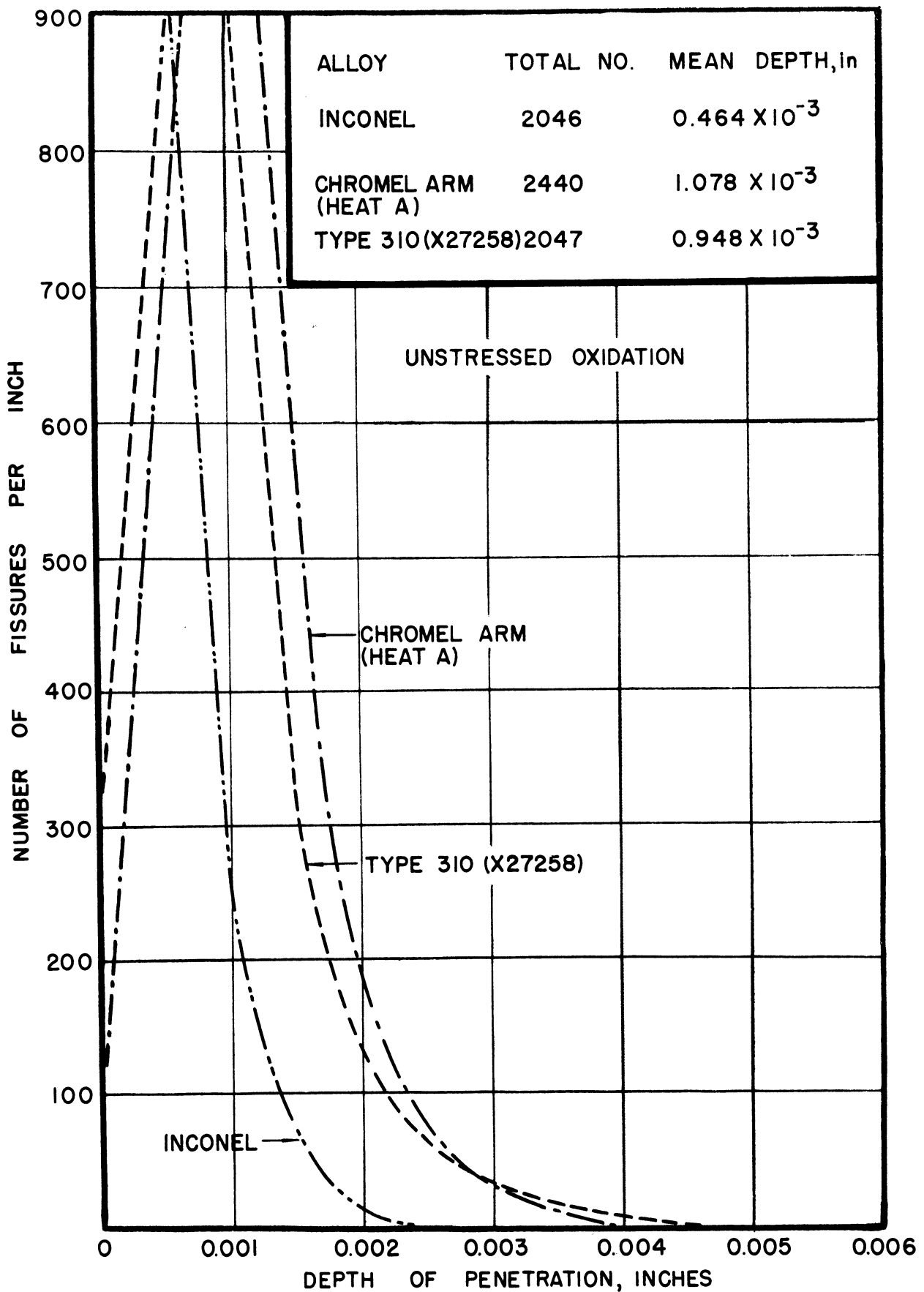


FIG.33 - PENETRATION VS. DEPTH BELOW SURFACE.  
 INCONEL, CHROMEL ARM & TYPE 310 (X27258) ALLOYS.  
 1900°F. 500 HRS DURATION.

